Tsukuba Geoenvironmental Sciences, Vol. 11, pp. 13-20, Dec. 25, 2015

Measuring urban volume: geospatial technique and application

Ronald C. ESTOQUE*, Yuji MURAYAMA*, Takeo TADONO** and Rajesh B. THAPA**

Abstract

Geospatial techniques based on remote sensing and geographic information system (GIS) are important in urban studies. However, based on traditional techniques, the analysis of the intensity and spatial pattern of urban land use is, in most cases, based only on the lateral extent of built-up lands (two-dimensional). The increasing availability of geospatial data, such as remote sensing satellite imageries and digital surface models, provides an opportunity for the integration of the third dimension in urban analysis, i.e. height of urban features such as high-rise buildings, into urban studies, and thus enables the estimation of the so-called urban volume. This study introduces a geospatial technique for estimating urban volume, focusing on the use of a digital surface model (DSM) derived from ALOS PRISM data. It also presents a method for deriving a digital terrain model (DTM) from a DSM. The proposed technique was tested in Makati City, Metro Manila, Philippines. Overall, the results show that the proposed technique is capable of taking into consideration the height dimension in urban analysis. The proposed two-step grid-based method for deriving a DTM from a DSM is also implementable and promising. In this method, there is a need to calibrate the size of the mesh for identifying the pixels or points to be used in DTM interpolation. This is because different mesh sizes can produce substantially different DTMs, surface feature height values and urban volume estimates.

Key words: ALOS PRISM, DSM, DTM, GIS, remote sensing, urban volume

1. Introduction

Knowledge of urban forms, including intensity and spatial pattern of urban land use, is important in urban studies – urban morphology, urban geography, urban ecology and urban sustainability, among others. In general, urban development is sought for social and economic reasons. Consequently, urban development often leads to changes in the intensity at which the already existing urban fabric is used (Koomen *et al*. 2009). During urban development process, high-rise buildings are often built for various uses and purposes, such as condominiums/apartments, offices, hotels and commercial facilities.

The emergence of land change science – a field of study that deals with the patterns, processes and impacts of land changes (Gutman *et al*. 2004; Rindfuss *et al*. 2004; Turner *et al*. 2007), and the advances in geospatial technologies, such as remote sensing and GIS, have been important in urban studies, e.g. monitoring and analysis of landscape changes due to urbanization. However, it should be noted that most studies on the geographical analysis of urbanization have focused on the lateral expansion of built-up lands (two-dimensional) (e.g. Thapa and Murayama 2011; Estoque and Murayama 2013, 2015; Bagan and Yamagata 2014). In most cases, two or more subsequent land-use/cover (LUC) maps are used to detect and analyze the growth or expansion of urban areas. In this type of analysis, the third dimension, i.e. height, is not taken into consideration.

In previous studies, individual address and postcode point-data have been used to characterize urban land use intensity (Longley and Mesev 2002; Batty *et al*. 2004). However, it has also been pointed out that such techniques fail to take into account the importance of the third dimension in urban analysis (Batty *et al*. 2004). High-rise and voluminous buildings characterize economic dominance and power, high-density zones, business centers and economically active areas. However, without additional data on the third dimension, these studies fail to capture such important features (Koomen *et al*. 2009).

The analysis of the third dimension of urban morphology is scarce, mainly due to limited data availability (Koomen *et al*. 2009). However, the increasing availability of geospatial data, such as remote sensing satellite imageries and digital surface models, provides an opportunity to integrate the third dimension into urban studies, and thus enables the estimation of the so-called urban volume. In this paper, urban volume refers to the volume of an urban area based on its built-up features such as buildings.

In fact, there are still very few studies on urban volume using remote sensing data and geospatial techniques. Koomen *et al*. (2009) presented an approach for estimating urban volume based on elevation and vector layer (topographic) datasets. Santos *et al*. (2013) used LiDAR and other altimetric and planimetric data to characterize urban volumetry. The use of LiDAR data is also becoming popular in the field of urban green volume estimation (e.g.

* Faculty of Life and Environmental Sciences, University of Tsukuba, Japan
** Japan Aerospace Exploration Agency, Japan

Hecht *et al*. 2008; Huang *et al*. 2013). However, the availability of high spatial resolution data, including LiDAR data, across different urban landscapes is very limited. Furthermore, a methodological framework for estimating urban volume from non-LiDAR data is still lacking. Hence, this study introduces a geospatial technique for such a purpose, focusing on the use of a digital surface model (DSM) derived from ALOS PRISM data. It also presents a method for deriving a digital terrain model (DTM) from a DSM.

2. Methodology

2.1. Study area and data used

For the purpose of this study, a 10 km × 10 km subset of Metro Manila, Philippines, covering Makati City was used as a test site. Makati City is the financial center of the Philippines. It has the highest concentration of high-rise buildings in the country, which are used by various local and multinational corporations.

The data used in this study include a multispectral satellite image (Landsat image acquired in 2009) and a DSM. The DSM was derived from the Advanced Land Observing Satellite 'DAICHI' or ALOS-1 PRISM data (2006-2011) (Tadono *et al*. 2014; Takaku *et al*. 2014). The Landsat image, with a spatial resolution of 30 m, was obtained from the United States Geological Survey (USGS) (http://earthexplorer.usgs.gov/), while the ALOS PRISM DSM (c. 2009), with a spatial resolution of 5 m, was obtained from the Japan Aerospace Exploration Agency (JAXA). Fig. 1 shows the ALOS PRISM DSM and the classified built-up/non-built-up maps of the test study site. The extraction of built-up and non-built-up classes from the Landsat image is described in section 2.2. A high spatial resolution satellite image was preferred, but due to limitations on data availability, a medium spatial resolution satellite image was used instead.

2.2. Built-up/Non-built-up mapping

The Landsat ETM+ image (surface reflectance data with Landsat Scene ID LE71160502009064EDC00; 5 March, 2009) used in this study was a pre-processed data (http://earthexplorer.usgs.gov/). During pre-processing by the USGS, the image went through the process of radiometric calibration and atmospheric correction (http://landsat.usgs.gov/CDR_LSR.php). However, because the image was not gap-filled during the surface reflectance production process, gap filling was undertaken following the procedure for filling gaps for scientific analysis (Erdas Imagine-Mosaicking Method, http://landsat.usgs.gov/sci_an.php). The clouds were also clipped and filled. The Landsat ETM+ image used as filler was also a pre-processed surface reflectance data (with Landsat Scene ID LE71160502008078EDC00; 18 March, 2008). The issue on seasonality and data quality and availability were considered in the selection of the filler image.

The final pre-processed image, in its original spatial resolution of 30 m, was classified using maximum likelihood supervised classification technique. This technique involves the digitizing of training sites or samples (e.g. built-up 1, 2,... n, and non-built-up 1, 2,... n) and using these samples to train and eventually classify the pixels in the image (Estoque and Murayama 2013). To produce a built-up/non-built-up map, the classified built-up and non-built-up pixels based on the training samples were merged. The built-up/non-built-up map had an overall accuracy of 88.89%.

Furthermore, the built-up/non-built-up map was resampled to 5 m using nearest neighbor algorithm, following the spatial resolution of the ALOS PRISM DSM (Fig. 2). This approach enabled further processing, while retaining the original information in the DSM and built-up/non-built-up maps.

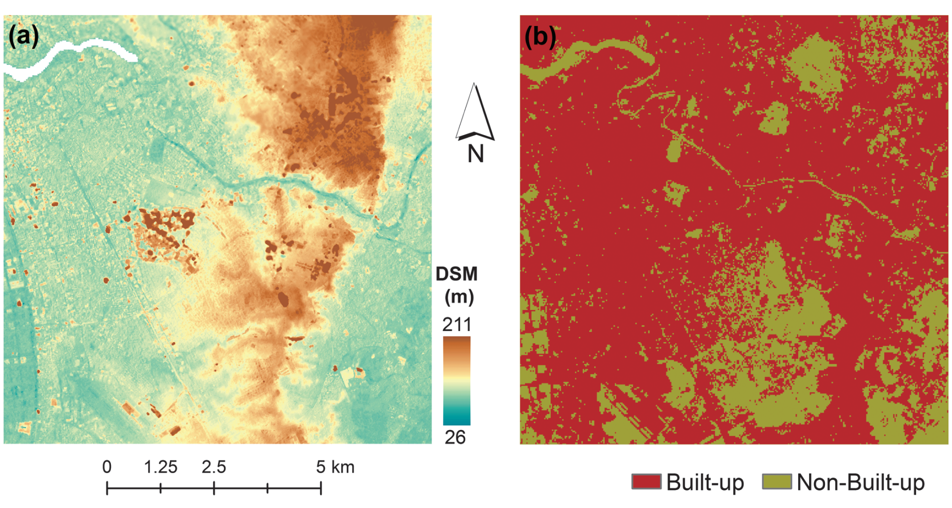

Fig. 1 The (a) ALOS PRISM DSM and (b) built-up/non-built-up maps of the test study site.

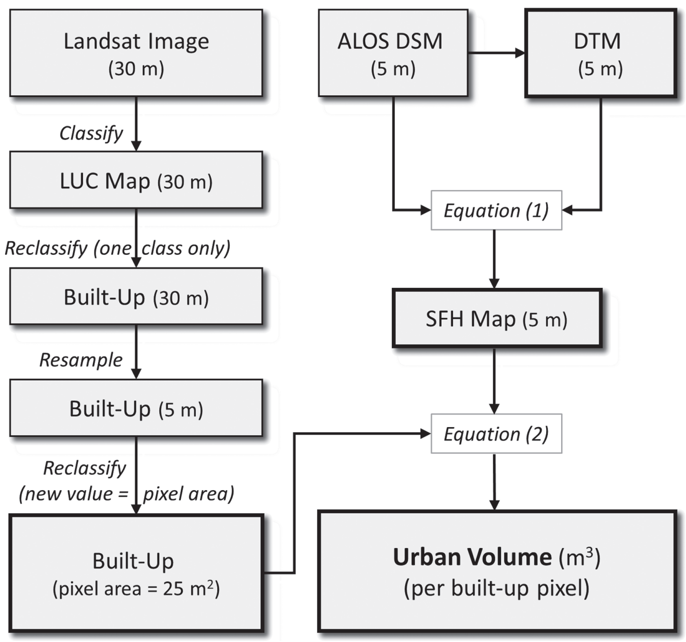

Fig. 2 Flowchart of the proposed geospatial technique for estimating urban volume from remote sensing data.

2.3. DTM derivation

Another core component of the proposed technique for estimating urban volume is the derivation of a DTM from a DSM (Fig. 2). Fig. 3 shows a graphical illustration of the ALOS PRISM DSM. In the illustration, the DSM value of hypothetical building x equals the sum of A, B, and C, which is also equal to the sum of C and D.

The idea is to derive the topographic surface (brown line in Fig. 3, online version), herein referred to as the DTM, from the ALOS PRISM DSM. This study hypothesizes that if the DTM can be derived, the height of surface features, like the hypothetical building x (i.e. labelled C in Fig. 3), from the ground (topographic surface) up to the top can also be determined. In this paper, this height is referred to as the surface feature height (SFH). However, the challenge centers on how to determine or approximate the DTM value of a topographic surface, especially those occupied by buildings, like the hypothetical building x.

In this study, we proposed a two-step grid-based method for deriving a DTM from a DSM: (1) sample points identification, and (2) surface interpolation. Let us assume that Fig. 4a is a cross section of a 300-m hypothetical urban landscape. The idea is to identify and locate the point (or pixel in the DSM map) with the lowest DSM value within a grid (e.g. 100-m grid). Fig. 4b shows the pixel with the lowest DSM value within a 100-m grid. In this study, various grid or mesh sizes were examined (i.e. 100 m, 150 m, 200 m, 250 m, 300 m, 350 m, and 400 m). The identified sample points for each mesh size were used in the DTM interpolation, employing the Empirical Bayesian Kriging approach (Krivoruchko 2012). The process produced seven DTMs, i.e. DTM100, DTM150, and so on.

2.4. Surface feature height (SFH) and urban volume measurement

The next step in the process before urban volume can be estimated involves the production of a SFH map (Fig. 2). Since there were seven derived DTMs, seven SFH maps were also produced (Eq. (1); Fig. 2) (SFH100, SFH150, and so on).

$$\text{SFH (m)} = \text{DSM} - \text{DTM} \qquad (1)$$

Using the map containing the extracted built-up pixels (pixel value = pixel area = 25 m^2) and the derived SFH maps, seven urban volume (UV) (m^3) maps of the test study site were produced (Eq. (2); Fig. 2) (UV100, UV150, and so on).

$$UV_i\ (m^3) = PA_i \times SFH_i \qquad (2)$$

where UV_i, PA_i and SFH_i are, respectively, the urban volume (m^3), area (m^2) and surface feature height (m) of pixel i, where pixel i is a member of the built-up class.

3. Results and Discussion

3.1. Derived DTMs

The derived DTMs had values ranging from 26 m to 91-155 m (Fig. 5). The interpolation process had a root mean square error ranging from 0.372 m (for DTM150) to 0.599 m (for DTM400). Smaller mesh sizes produced more sample points than the larger mesh sizes. This explains the dif-

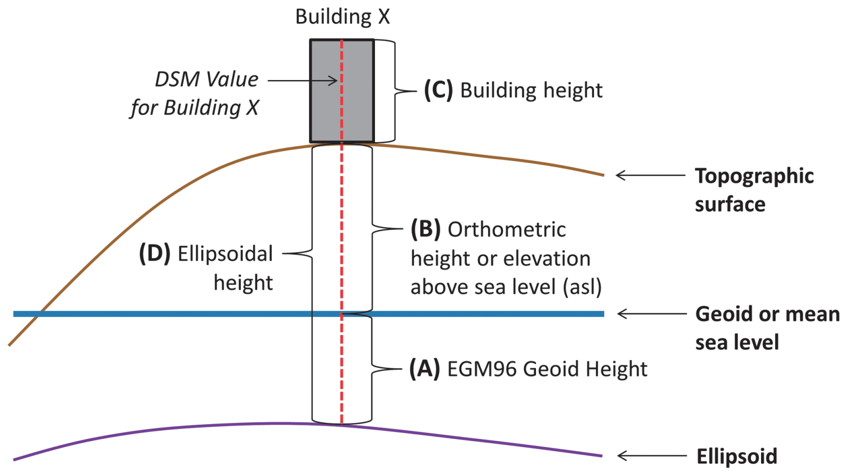

Fig. 3 Illustration of the ALOS PRISM DSM, highlighting the DSM value of hypothetical building x (DSM = A+B+C = C+D). Coordinate system/Ellipsoid model: ITRF97/GRS80.

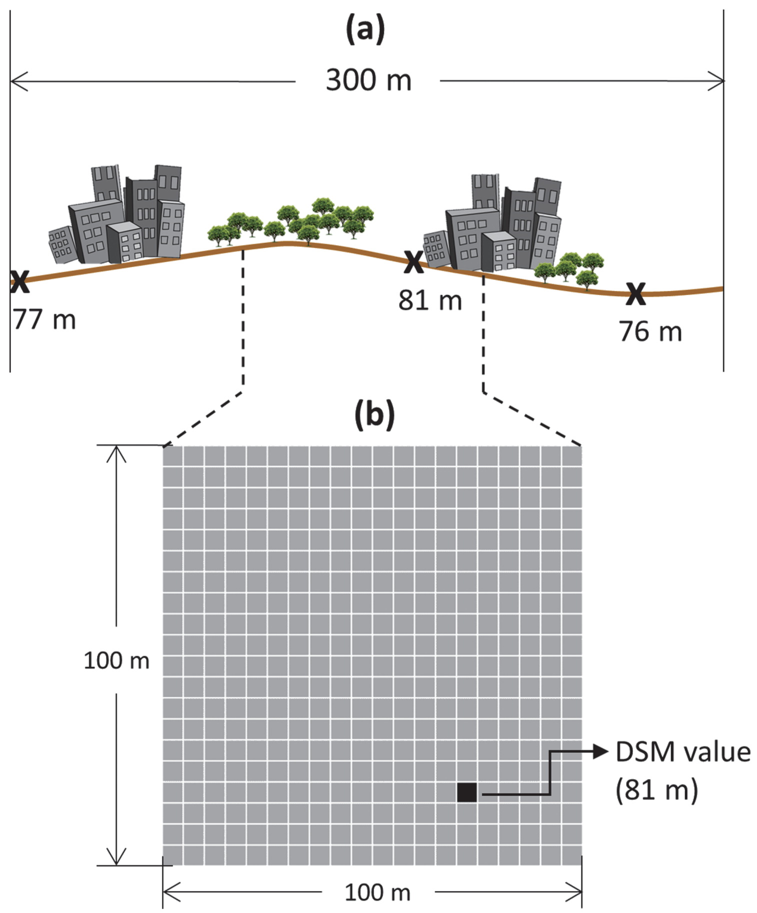

Fig. 4 Illustration of the collection of sample points for deriving a DTM from a DSM using a grid-based method. (a) cross section of a 300-m hypothetical urban landscape; and (b) a 100-m grid showing the hypothetical pixel with the lowest DSM value.

ference in the value ranges of the derived DTMs. It can also be observed that smaller mesh sizes (with more sample points), also produced finer or more detailed DTMs, while larger mesh sizes produced coarser and more generalized DTMs. However, the question is 'did the smaller mesh sizes also produce more accurate DTMs?' Due to the lack of reference data that is more accurate than the derived DTMs, we could not quantify the respective accuracy of the derived DTMs. Nevertheless, to help determine which DTM is likely more accurate, we paid closer attention to the derived SFH maps.

3.2. Derived SFH maps

The results show that the derived SFH maps also had different value ranges. This was due to the input DTMs. The minimum SFH value ranges from -28.2 m (SFH100) to -10.3 m (SFH200), while the maximum SFH value ranges from 137.5 m (SFH100) to 149.4 m (SFH350) (Fig. 6). Since the DSM values of built-up features, like the hypothetical building x in Fig. 3, are supposedly higher than their respective DTM values (topographic surface, brown line in Figs. 3 and 4a, online version), pixels with negative SFH values can be considered errors. Among the seven derived SFH maps, SFH100 had the highest quantity of pixels with negative SFH values, while SFH300 had the lowest (Fig. 6). Based on the quantity of pixels that are in conflict with the premise DSM > DTM, SFH300 can be considered the most accurate among all seven SFH maps.

3.3. Estimated urban volume

The different SFH maps (Fig. 6), produced using different DTMs (Fig. 5), also produced different urban volume

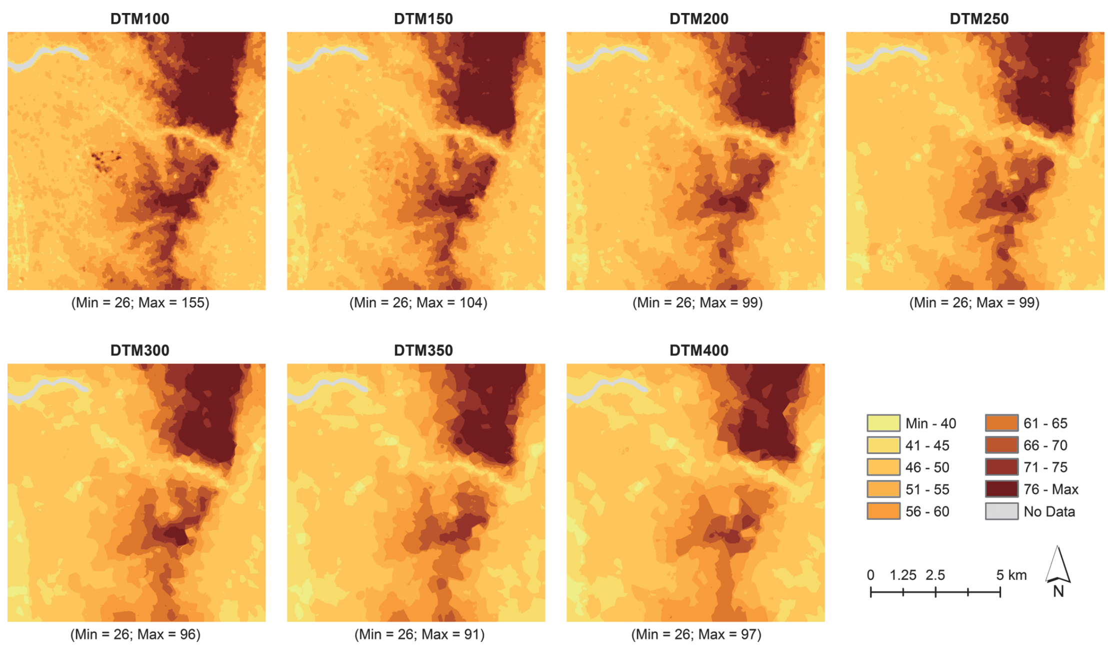

Fig. 5 The DTMs (m) derived from the ALOS PRISM DSM using the two-step grid-based method (section 2.3).

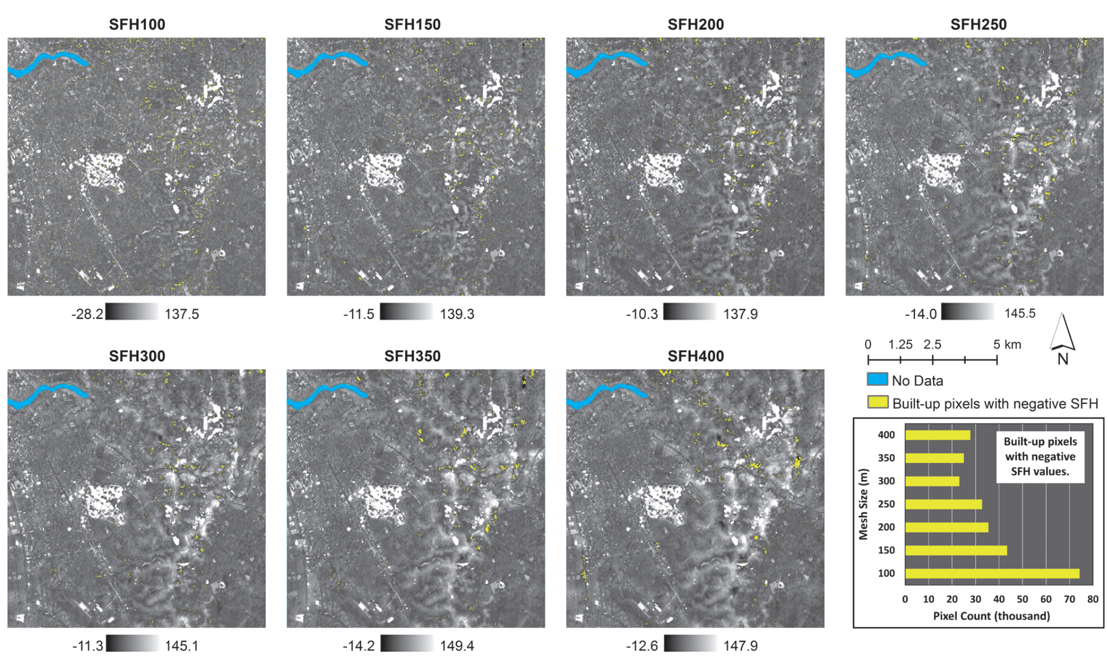

Fig. 6 The SFH maps (m) produced using the ALOS PRISM DSM and the seven derived DTMs.

estimates (Fig. 7). The maximum urban volume value ranges from 3439 m^3 (UV100) to 3736 m^3 (UV350) (Fig. 7). It can be observed that the urban volume maps produced using larger mesh sizes (for collecting sample points for DTM interpolation) had more dark pixels, indicating that they had higher estimates of urban volume. This is because the larger mesh sizes also produced lower DTM values (Fig. 5) and higher SFH values (Fig. 6). Based on UV300, produced by SFH300, the test study site had a total urban volume of 618.74 million m^3. This translates to an urban volume index of 61,874.2 m^3 per ha.

The estimated urban volume of the test study site can be used to indicate the degree of urban land use intensity and pattern in the area. It can be observed that the intensity and pattern of urban land use is not uniformly distributed across the whole area. There are hot spots (high urban volume) and cold spots (low urban volume). The comparison between UV300 and a Google Earth image is shown in Fig. 8. The comparison shows that the spatial distribution of high-rise buildings in the test study site as shown in the

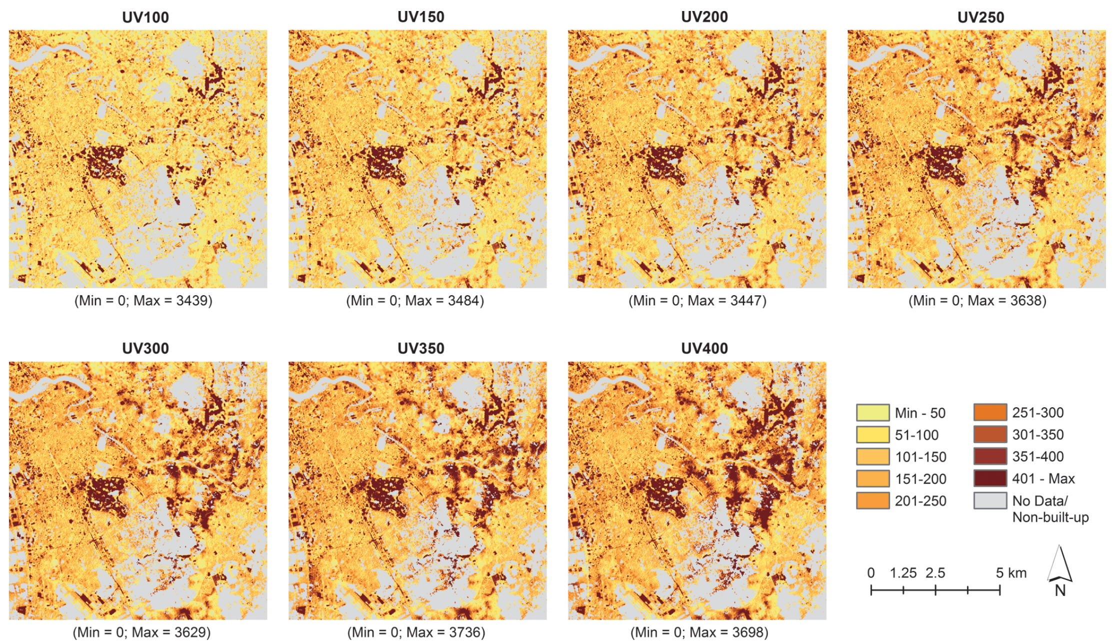

Fig. 7 The urban volume (UV) maps (m^3) of the test study site. Built-up pixels with negative SFH values were not included in the calculation.

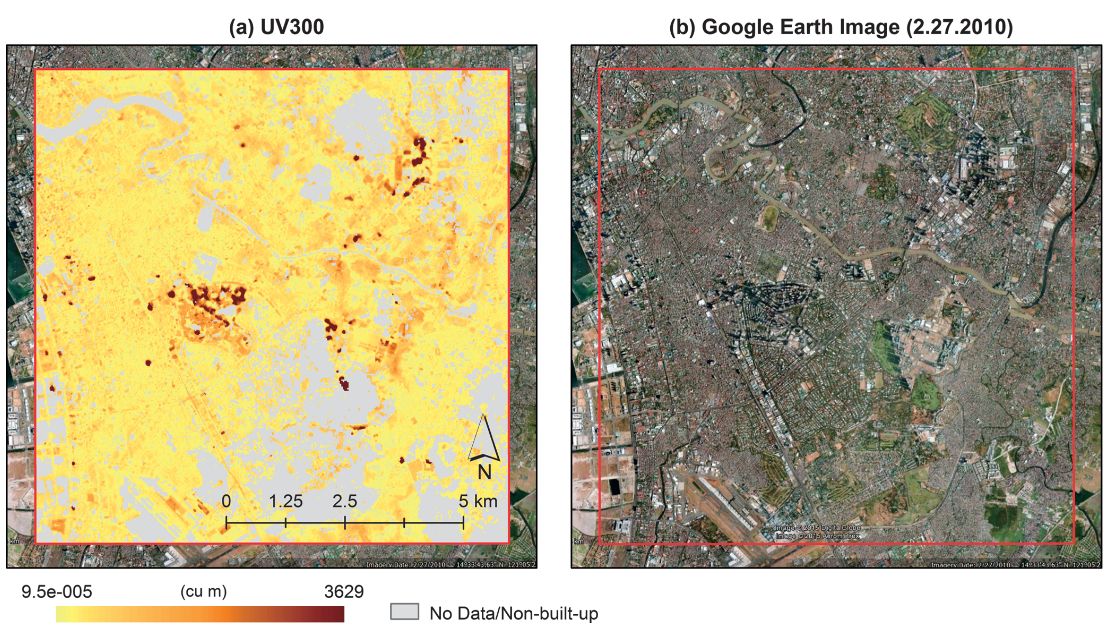

Fig. 8 Comparison between (a) UV300 (c. 2009) and (b) Google Earth image (2010).

reference image mirrors the spatial distribution of pixels with higher urban volume estimates (dark pixels in UV300 map). This indicates a certain degree of confidence on the estimated urban volume of the test study site, in particular, and on the proposed technique for urban volume estimation, in general.

3.4. Relevance of urban volume in urban studies

The characterization and analysis of urban forms, including intensity and spatial pattern of urban land use, is important in urban studies (e.g. urban geography and urban morphology) (Longley and Mesev 2002; Batty *et al*. 2004; Koomen *et al*. 2009; Estoque and Murayama 2015). In this study, urban volume, which is based on built-up volume, has been used as a proxy measure for characterizing and examining the intensity and spatial pattern of urban land use in Makati City, Metro Manila. Urban volume can also be used as a proxy indicator for characterizing social structure, intensity of economic activity, relative levels of economic supremacy and power, as well as relative resource consumption levels, across various units of analysis. In addition, we postulate that urban volume can also be used as an indicator or parameter in urban ecological studies. For example, the spatial distribution of urban ecosystem services can be examined in relation to urban volume. Urban volume can also be used in the context of urban heat island studies. A time-series urban volume analysis can also provide new perspectives in urban studies. Hence, once multi-temporal DSM data become available, it is also important to add the time dimension in the analysis, e.g. spatiotemporal analysis of urban volume.

4. Conclusions and future prospects

Overall, the results show that the proposed geospatial technique for estimating urban volume is capable of taking into consideration the height dimension in urban analysis. The proposed two-step grid-based method for deriving a DTM from a DSM is also implementable and promising. In this method, there is a need to calibrate the size of the mesh for identifying the pixels or points to be used in DTM interpolation. This is because different mesh sizes can produce substantially different DTMs, SFH values and urban volume estimates. The future prospects of this study include the development of validation methods for the estimated urban volume, implementation of the proposed technique in other cities, including Bangkok and Jakarta, as well as the integration of high spatial resolution satellite imageries as sources of built-up footprints.

Acknowledgements

This study was supported by the Japan Society for the Promotion of Science through Grant-in-Aid for Scientific Research B: No. 26284129, 2014-16 (Representative: Yuji Murayama), A: No. 24241053, 2013-16 (Representative: Tsutomu Suzuki) and Grant-in-Aid for Research Activity Start-Up: No. 15H06067 (Representative: Ronald C. Estoque).

References

Bagan, H. and Yamagata, Y. (2014): Land-cover change analysis in 50 global cities by using a combination of Landsat data and analysis of grid cells. *Environmental Research Letters*, **9**, 064015.

Batty, M., Besussi, E., Maat, K. and Harts, J.J. (2004): Representing multifunctional cities: density and diversity in space and time. *Built Environment*, **30**, 324–337.

Estoque, R.C. and Murayama, Y. (2013): Landscape pattern and ecosystem service value changes: implications for environmental sustainability planning for the rapidly urbanizing summer capital of the Philippines. *Landscape and Urban Planning*, **116**, 60–72.

Estoque, R.C. and Murayama, Y. (2015): Intensity and spatial pattern of urban land changes in the megacities of Southeast Asia. *Land Use Policy*, **48**, 213–222.

Gutman, G., Janetos, A.C., Justice, C.O., Moran, E.F., Mustard, J.F., Rindfuss, R.R., *et al*. (2004): *Land change science: observing, monitoring and understanding trajectories of change on the Earth's surface*. Kluwer Academic, New York, 459p.

Hecht, R., Meinel, G. and Buchroithner, M.F. (2008): Estimation of urban green volume based on single-pulse LiDAR data. *IEEE Transactions on Geoscience and Remote Sensing*, **46**, 3832–3840.

Huang, Y., Yu, B., Zhou, J., Hu, C., Tan, W., Hu, Z. and Wu, J. (2013): Toward automatic estimation of urban green volume using airborne LiDAR data and high resolution remote sensing images. *Frontiers of Earth Science*, **7**, 43–54.

Koomen, E., Rietveld, P. and Bacao, F. (2009): The third dimension in urban geography: the urban-volume approach. *Environment and Planning B: Planning and Design*, **36**, 1008–1025.

Krivoruchko, K. (2012): *Empirical Bayesian kriging: implemented in ArcGIS geostatistical analyst*. ESRI, Redlands, CA, USA. Available online: http://www.esri.com/news/arcuser/1012/files/ebk.pdf (Last accessed 11 November 2015).

Longley, P.A. and Mesev, V. (2002): Measurement of density gradients and space-filling in urban systems. *Papers in Regional Science*, **81**, 1–28.

Rindfuss, R.R., Walsh, S.J., Turner, B.L. II., Fox, J. and Mishra, V. (2004): Developing a science of land change: challenges and methodological issues. *Pro-*

ceedings of the National Academy of Sciences of the USA, **101**, 13976–13981.

Santos, T., Rodriguez, A.M. and Tenedorio, J.A. (2013): Characterizing urban volumetry using LiDAR data. *International Archives of the Photogrammetry, Remote Sensing and Spatial Information Sciences*, **XL-4/W1**, 71-75.

Tadono, T., Ishida, H., Oda, F., Naito, S., Minakawa, K. and Iwamoto, H. (2014): Precise global DEM generation by ALOS PRISM. *ISPRS Annals of the Photogrammetry, Remote Sensing and Spatial Information Sciences*, *II-4*, 71–76.

Takaku, J., Tadono, T. and Tsutsui, K. (2014): Generation of high resolution global DSM from ALOS PRISM. *The International Archives of the Photogrammetry, Remote Sensing and Spatial Information Sciences*, **XL-4**, 243–248.

Thapa, R.B. and Murayama, Y. (2011): Urban growth modeling of Kathmandu metropolitan region, Nepal. *Computers, Environment and Urban Systems*, **35**, 25–34.

Turner, B.L. II., Lambin, E.F. and Reenberg, A. (2007): The emergence of land change science for global environmental change and sustainability. *Proceedings of the National Academy of Sciences of the USA*, **104**, 20666–20671.

Received 10 September 2015
Accepted 5 November 2015